Science of the Total Environment 888 (2023) 163888

Contents lists available at ScienceDirect

Science of the Total Environment

journal homepage: www.elsevier.com/locate/scitotenv

Effects of high pressure and temperature conditions on the chemical fate of flowback water related chemicals

Ann-Hélène Faber [a,b,c,e,*], Andrea M. Brunner [b,f], Mariska Schimmel [d,g], Paul P. Schot [a], Pim de Voogt [b,c], Annemarie van Wezel [c]

[a] Copernicus Institute of Sustainable Development, Faculty of Geosciences, Utrecht University, Utrecht, the Netherlands
[b] KWR Water Research Institute, Nieuwegein, the Netherlands
[c] Institute for Biodiversity and Ecosystem Dynamics, University of Amsterdam, Amsterdam, the Netherlands
[d] HPT Laboratory, Department of Earth Sciences, Faculty of Geosciences, Utrecht University, Utrecht, the Netherlands
[e] Administration de la Gestion de l'Eau, Esch-sur-Alzette, Luxembourg
[f] TNO, Environmental Modelling Sensing and Analysis, Utrecht, the Netherlands
[g] Ministry of Economic Affairs and Climate Policy, The Hague, the Netherlands

HIGHLIGHTS

- Are current environmental fate models suitable for downhole activities?
- Chemical comparison of high pressure/temperature and atmospheric samples
- Chemical composition analysed via non-target screening using LC-HRMS
- Average change is equal or lower to a factor 5.
- Use of environmental fate models possible using additional factor of 5

GRAPHICAL ABSTRACT

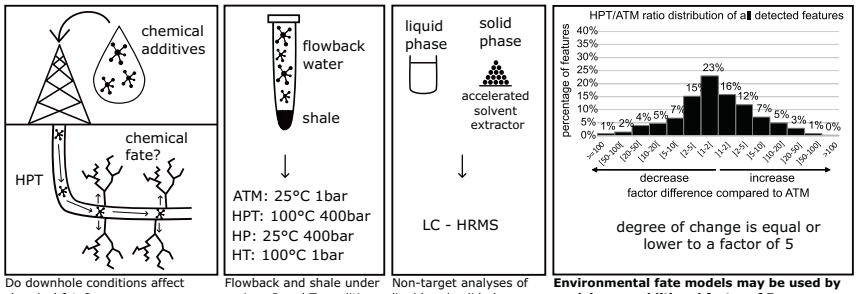

ARTICLE INFO

Editor: Daniel Alessi

Keywords:
Downhole conditions
Environmental fate
Risk assessment
Flowback water
Shale

ABSTRACT

Environmental risk assessment is generally based on atmospheric conditions for the modelling of chemical fate after entering the environment. However, during hydraulic fracturing, chemicals may be released deep underground. This study therefore focuses on the effects of high pressure and high temperature conditions on chemicals in flowback water to determine whether current environmental fate models need to be adapted in the context of downhole activities. Crushed shale and flowback water were mixed and exposed to different temperature (25–100 °C) and pressure (1–450 bar) conditions to investigate the effects they have on chemical fate. Samples were analysed using LC-HRMS based non-target screening. The results show that both high temperature and pressure conditions can impact the chemical fate of hydraulic fracturing related chemicals by increasing or decreasing concentrations via processes of transformation, sorption, degradation and/or dissolution. Furthermore, the degree and direction of change is chemical specific. The change is lower or equal to a factor of five, but for a few individual compounds the degree of change can exceed this factor of five. This suggests that environmental fate models based on surface conditions may be used for an approximation of chemical fate under downhole conditions by applying an additional factor of five to account for these uncertainties. More accurate insight into chemical fate under downhole conditions may be gained by studying a fluid of known chemical composition and an increased variability in temperature and pressure conditions including concentration, salinity and pH as variables.

* Corresponding author at: Copernicus Institute of Sustainable Development, Faculty of Geosciences, Utrecht University, Utrecht, the Netherlands.
E-mail address: annhelene.faber@gmail.com (A.-H. Faber).

http://dx.doi.org/10.1016/j.scitotenv.2023.163888
Received 30 December 2022; Received in revised form 21 April 2023; Accepted 27 April 2023
Available online 8 May 2023

1. Introduction

Hydraulic fracturing is a well stimulation technique used to extract oil and/or gas from impermeable rock formations, such as sandstone or shale. For one hydraulic fracture, approximately 10 million litres of fracturing fluid made up of 90 % water, 9 % proppants and 1–2 % chemical additives may be injected into the formation at high pressure (Vidic et al., 2013; Sun et al., 2019). As soon as the pressure is released, wastewater known as flowback water and produced water makes its way up together with oil and/or gas through the well. Flowback water flows up to the surface in the first few days after fracturing has taken place, followed by produced water. Flowback water mainly contains the initially injected hydraulic fracturing fluid whereas produced water is mainly made up of oil and/or gas and the mobilised geogenic chemicals (Blewett et al., 2017; Wang et al., 2019; Zhou et al., 2022). The wastewater is separated from the oil and gas and is then generally disposed of via deep-well injection or recycled for re-use, with an emphasis on wastewater reuse due to the high demand of freshwater and the related sustainability concerns (Seth et al., 2013; Boschee, 2014; Ellafi et al., 2020; Hernández-Pérez et al., 2022).

Flowback water contains the initially injected chemical additives, chemicals that were present in the formation and mobilised during the hydraulic fracturing process, and transformation products of those chemicals (Sun et al., 2019). Chemical additives used in fracturing fluid typically include biocides, scale and corrosion inhibitors, cleaners, gelling agents, surfactants, cross-linkers and breakers (Faber et al., 2017; Reynolds, 2020; Othman et al., 2021). The exact composition of a given fracturing fluid depends on the water quality used for injection and the local geological conditions. The chemicals originating from the subsurface strongly depend on the formation being fractured and may include heavy metals, radionuclides, salts and hydrocarbons.

During hydraulic fracturing, contamination of freshwater or groundwater may occur due to accidental aboveground spills or belowground leaks, resulting from structural integrity failure of the well and the underground formations (Gordalla et al., 2013; Schimmel et al., 2019; Schout et al., 2019; Yazdan et al., 2020; Jin et al., 2022). Failure probabilities are rather low, i.e. 0.0002–1.6 %/well/year, depending on the contamination pathway and the fluid involved (Faber et al., 2017), nevertheless these still arise. Contaminations of groundwater and drinking water have been recorded as a result of hydraulic fracturing-related activities (Osborn et al., 2011; Fontenot et al., 2013; Gross et al., 2013; Preston and Chesley-Preston, 2015; Faber et al., 2017; Brantley et al., 2018; Missimer and Maliva, 2020; Rodriguez et al., 2020; Turley and Caretta, 2020; Wollin et al., 2020; Yadav et al., 2020; Bonetti et al., 2021; Casey et al., 2022). Therefore, environmental risk assessment of hydraulic fracturing activities is needed to ensure the safety of human and environmental health.

In chemical risk assessment, exposure concentrations in the different compartments (water, soil and air) are calculated based on environmental fate properties using conceptual box models, such as Simplebox (Hollander et al., 2016; Thunnissen et al., 2020); Wang et al., 2020a; Qu et al., 2022) or QWASI (Mackay et al., 1983; Wang et al., 2020b; Wang et al., 2023). These models are generally based on aboveground emission routes as well as atmospheric conditions (Suciu et al., 2013; Mansouri et al., 2018; Di Guardo et al., 2018; Tong et al., 2022). However, during hydraulic fracturing, chemicals may be released deep underground. At a depth of 4 km, temperatures rise to around 100 °C and pressure to around 450 bar. Thus, in order to adequately predict where additives and other constituents of the flowback water are most likely to end up in the environment, whether transformation occurs and what concentrations result from the chemical processes that take place underground, more information on chemical behaviour under downhole conditions is needed. If downhole conditions have a negligible effect on chemical fate, currently used box models may be used to assess exposure. However, if downhole conditions significantly affect chemical fate compared to aboveground atmospheric conditions the models would need to be revised (Faber et al., 2017). At current limited information is available on this subject. Kahrilas et al. (2015, 2016) published a literature review focusing on biocides, and a research paper on downhole transformation of glutaraldehyde. The experimental conditions included temperatures of 65 to 140 °C, pressures of 6.9 to 110 bar, pH of 6 to 8 and salinity of 0 to 2.8 M [NaCl], and found that downhole conditions did alter chemical behaviour and that temperature, pH and salinity had the greatest effect, while the effects of pressure were negligible.. Tasker et al. (2016) studied the effects of high pressure (83 bar) and temperature (80 °C) conditions on organic compounds and found that temperature and pressure greatly affected the organic composition of a synthetic fracturing fluid. It should however be noted that temperature and pressure were studied as one variable. Xiong et al. (2018) examined the effects of downhole conditions (80 °C, 83 bar and 3 M [NaCl]) on polyacrylamide degradation and noted that degradation of polyacrylamide was impacted by high temperatures whereas pressure and salinity did not play a role. Schenk et al. (2019) investigated the leaching of formaldehyde and other leachates from proppants under high temperature conditions (93 °C) and found that temperature influences leaching of formaldehyde and other leachates from proppants. This study, however, did not consider the effects of pressure. Song et al. (2022) researched the solubility of methane in oil-based mud under high temperature (40–140 °C) and pressure (20–560 bar) conditions and found that pressure had a greater effect on methane solubility in oil-based muds than temperature did. All these studies limited their focus on the behaviour of a single specific chemical or a group of chemicals (i.e. metals).

In this study we therefore investigate the effects of high pressure and temperature conditions on the fate of a broad selection of chemicals present in flowback water. We used liquid chromatography coupled to high resolution mass spectrometry (LC-HRMS) based non-target screening (Hollander et al., 2016; Hajeb et al., 2022; Tisler and Christensen, 2022) with a focus on the polar organic chemicals, which are of most concern to water quality due to their low removal efficiencies during wastewater treatment (Westerhoff et al., 2005; Reemtsma et al., 2016; Hale et al., 2020). Salinity, pH and organic content were not taken into account. Based on our findings, we analyse the applicability of commonly used environmental fate models to evaluate risks of chemicals in shale gas exploration and exploitation.

2. Methods and materials

2.1. Scientific approach

Crushed shale (< 2 mm) and flowback water were mixed and tested under different temperature and pressure conditions to determine the effects on chemical fate. In this study chemical fate relates to where the chemical ends up, whether transformation occurred and what concentrations are found. The experimental conditions include a high pressure and high temperature (HPT) condition (100 °C, 450 bar), a high temperature (HT) condition (100 °C, 1 bar), a high pressure (HP) condition (25 °C, 450 bar) and an atmospheric (ATM) condition (25 °C, 1 bar). The HPT condition simulates conditions around a depth of 4 km. Chemical analyses using LC-HRMS screening provide information on the chemicals present both in the liquid phase (i.e. flowback fluid) and the solid phase (i.e. the crushed shale) under the different conditions.

2.2. Materials

The shale was obtained from a Dutch Posidonia shale formation (Van Bergen et al., 2013; Amberg et al., 2022) taken at a 900 m depth and was supplied by the TNO core storage centre in Zeist, the Netherlands. The shale (S) was crushed using a centrifuge mill and subsequently sieved over a 2 mm round sieve. The flowback water (FBW) originated from a Baltic shale gas basin in Poland and was supplied under a non-disclosure agreement concerning the location and the composition of the fracturing fluid used at the site Butkovskyi et al., 2018. The flowback water was collected in 20 L plastic containers and transported to KWR Water Research Institute in the Netherlands, where it was stored at 4 °C until the start of the experiments. The flowback water had a relatively high salinity (103 g/L total dissolved solids), dissolved organic carbon (649 mg/L), and chemical oxygen

demand (1800 mg/L), and a relatively low pH (4.9) (Butkovskyi et al., 2018). For the experiments, 8 mL Teflon tubes with screw caps were used. The lining of the Teflon tube walls were thinned over a length of 1 cm, so that the effects of the pressure may be exerted on the contents of the tube (Fig. A.1). Acetonitrile (ACN, HPLC grade) was purchased from Avantor Performance Materials B.V. (Deventer, The Netherlands), formic acid (FA) from Fluka Analytical (Sigma-Aldrich, Steinheim, Germany), and the internal standards atrazine-d_5 and bentazone-d_6 were ordered from CDN isotopes (Pointe-Claire, Canada) and from LGC (Almere, The Netherlands), respectively. An Elga Purelab Chorus ultrapure water system (High Wycombe, UK) was used to produce ultrapure water (UPW).

2.3. Sample preparation and experimental conditions

For each of the four conditions, one test sample and three separate control samples were prepared. All samples were prepared in triplicate in the modified Teflon tubes placed in a glovebox to stimulate anoxic downhole conditions. The test samples (FBW + S) contained 500 mg of crushed shale and 7.5 mL of four times diluted flowback water, control 1 (UPW) contained 8 mL of ultrapure water, control 2 (FBW) contained 8 mL of four times diluted flowback water, and control 3 (UPW + S) contained 500 mg of crushed shale and 7.5 mL of ultrapure water. Table 1 provides an overview of the test samples and controls. The flowback water was diluted to avoid expansion and bursting of the tube when exposed to the high temperatures. The expansion and bursting of the tube seems probable because the flowback water contains volatile compounds that evaporate at higher than atmospheric temperatures, which exerts pressure on the tube and can cause it to burst. The diluted flowback water contains fewer volatile compounds, which results in a lower pressure build up.

The 500 mg crushed shale was weighed individually for each sample before placing them in the glovebox. Helium was then slowly blown through the samples to facilitate reaching anoxic conditions in the glovebox. All materials and tools were put in the glovebox at least 4 h prior to preparing the samples until anoxic conditions were reached. The diluted flowback or ultrapure water mixture was added to the tubes and mixed using a glass rod. The tubes were then tapped to remove all air bubbles. The tubes were then sealed by slightly pressing on opposite sides of the tube to avoid air being trapped inside. The experimental conditions for the HPT and HP samples were carried out in a pressure vessel at the HPT Laboratories at Utrecht University, The Netherlands. This vessel then builds up pressure by pumping silicon oil into the system, while heat can also be applied to increase temperature (Liteanu and Spiers, 2011). For the HT samples an oven placed in a fume hood was used, while ATM samples were placed in a fume hood.

1,2-benzisothiazolin-3-one is a white powder used as a corrosion inhibitor in hydraulic fracturing fluid (Faber et al., 2017). It is also used in industrial and consumer products for its antimicrobial properties (Haz-Map, 2021). 1,2-benzisothiazolin-3-one (2634-33-5) was added to each sample and control at a concentration of 2 mg/L. The purpose of the added chemical is not to be used as an internal standard but rather to semi-quantitatively evaluate the fate of a known chemical under the different pressure and temperature conditions.

2.4. Preparing the liquid and solid phases for HRMS analyses

After three days under the experimental HTP, HT, HP and ATM conditions, the samples were taken out. The HT and HPT samples were left to cool down for a short period of time to avoid injuries such as burning of hands during manipulation. The liquid phase was then separated from the solid phase using a syringe, filtered using a 0.2 μm syringe filter and stored in 10 mL glass vials in the freezer until analysis. The solid phase was vacuum filtered using a 55 mm microfiber glass filter (Whatman, Grade GF/A) and low vacuum. The shale containing filters were then left to dry before extraction using an accelerated solvent extractor (ASE 200 extractor, Dionex, USA). The fibreglass filters were weighed before adding the shale and after the shale had dried for three days to verify comparability among the samples. Methanol/Acetonitrile (1:1) was used as extraction solvent in the ASE with a pressure of 100 bar and a temperature of 100 °C. The ASE was run in two cycles per sample. Each cycle was programmed for 2 min of pre-heating, 5 min of heating, 10 min of static, followed by 60 % flush and 60 s purging. The extracts, containing 40 mL of fluid, were then evaporated under a steady flow of nitrogen in a fume hood until 1 mL of volume remained. 1 mL of ultrapure water was then added and the sample further evaporated until reaching 1 mL. This allowed for the transfer of chemicals from a methanol/acetonitrile matrix into a water matrix, which is more suitable for HRMS analyses. The vials containing the samples were weighed empty, before and after evaporation to determine accurate volumes during this process.

2.5. LC-HRMS analyses

The samples were analysed using LC-HRMS based non-target screening. The liquid phase samples and solid phase extracts were diluted 1000 and 10,000 times, respectively, using ultrapure water. All samples were then spiked with the internal standards atrazine-d_5 and bentazone-d_6 to a concentration of 100 μg/L to ensure quality control. A blank sample was also prepared containing ultrapure water and only the internal standard to follow and monitor the LC-HRMS analyses, in addition to the full procedural blank control. The samples were then analysed using an Orbitrap Fusion Tribrid mass spectrometer (Thermo Fisher Scientific, San Jose, USA) using a heated electrospray ionisation source coupled to a Vanquish HPLC system (Thermo Fisher Scientific). An XBridge BEH C18 XP column (150 mm × 2.1 mm I.D., 2.5 μm particle size, Waters, Etten-Leur, The Netherlands) in combination with a 2.0 mm × 2.1 mm I.D. Phenomenex

Table 1
Overview of test and control samples.

Sample abbreviation	Sample type	Condition	Content
ATM_FBW + S	Test	Atmospheric	7.5 mL flowback water and 500 mg shale
ATM_UPW	Control 1	Atmospheric	8 mL ultrapure water
ATM_FBW	Control 2	Atmospheric	8 mL flowback water
ATM_UPW + S	Control 3	Atmospheric	7.5 mL ultrapure water and 500 mg shale
HPT_FBW + S	Test	High pressure and temperature	7.5 mL flowback water and 500 mg shale
HPT_UPW	Control 1	High pressure and temperature	8 mL ultrapure water
HPT_FBW	Control 2	High pressure and temperature	8 mL flowback water
HPT_UPW + S	Control 3	High pressure and temperature	7.5 mL ultrapure water and 500 mg shale
HP_FBW + S	Test	High pressure	7.5 mL flowback water and 500 mg shale
HP_UPW	Control 1	High pressure	8 mL ultrapure water
HP_FBW	Control 2	High pressure	8 mL flowback water
HP_UPW + S	Control 3	High pressure	7.5 mL ultrapure water and 500 mg shale
HT_FBW + S	Test	High temperature	7.5 mL flowback water and 500 mg shale
HT_UPW	Control 1	High temperature	8 mL ultrapure water
HT_FBW	Control 2	High temperature	8 mL flowback water
HT_UPW + S	Control 3	High temperature	7.5 mL ultrapure water and 500 mg shale

Security Guard Ultra column (Phenomenex, Torrance, USA) was used at a temperature of 25 °C. The LC-HRMS method described by Brunner et al. (2020) was applied for non-target screening data acquisition.

2.6. Data analysis

The LC-HRMS raw data files were processed using Compound Discoverer 3.0 (Thermo Scientific, San Jose, USA) for peak picking, feature building and suspect screening. Features refer to pairs of retention time and accurate mass with a signal intensity. A feature intensity threshold >50,000 and a minimum of five times the blank was used for data processing. For suspect screening, a 5 ppm mass tolerance was applied in the searches of potential candidates against mzCloud (2019; HighChem LLC, Slovakia) and Chemspider (2019; Pence and Williams, 2010; Ayers, 2012; Habauzit et al., 2022; Mao et al., 2022) databases. The resulting feature list including a table with accurate masses, retention times and intensities reported as peak areas was exported to R Studio in the form of a .csv file for further data analysis and visualization (Table A.1ab, R Core Team, 2017). Feature intensities of the liquid and solid phase results were corrected for the intensities measured in the blanks and by applying the concentration or dilution factors resulting from sample preparation. Feature intensities were expressed as internal standard equivalent concentrations by using the known added concentrations of atrazine-d_5 and bentazone-d_6 for the positive and negative ionisation results, respectively. The number of detected features per sample was presented in the form of bar graphs. Ratio distributions of the HP, HT and HPT test samples compared to the ATM test samples were determined and plotted in the form of a bar graph against the percentage of detected features. The ratios were calculated based on IS-eq. concentrations of the features. Significant differences in feature intensities and number of detected features between the HPT, HP and HT conditions and the ATM conditions were determined based on a t-test (Tables A.3ab and A.4a-j). Violin plots were produced for insight into the retention time and molecular mass distribution, as well as feature intensity (Hintze and Nelson, 1998; Blumenschein et al., 2020; Hu, 2020). Principal component analysis (PCA) and hierarchical clustering were applied to characterise samples and features to reduce data complexity and reveal both similarities and differences between samples (Masiá et al., 2014; Köhn and Hubert, 2014; Jafarzadegan et al., 2019; Santos et al., 2019; Beattie and Esmonde-White, 2021; Li et al., 2022a). Cos2 was incorporated into the PCA analysis to show the importance of a principal component for a certain observation (Abdi and Williams, 2010; Li et al., 2022b). Significance testing and fold change filtering results were illustrated in Volcano plots displaying log2 fold change (log2FC) and the negative log 10-transformed p-values of features (Laplaza et al., 2022).

The top five features responsible for the main differences between the ATM samples and the HPT, HP and/or HT conditions were tentatively identified, using MS1 full scan and MS2 fragmentation data. MS1 data was used to elucidate the molecular formula of a feature and MS2 data to further identify a certain feature through comparing the experimental spectrum with an in silico generated spectrum using MetFrag (2020; Ruttkies et al., 2019; Schymanski et al., 2021). A scale defined by 5 levels of confidence (Schymanski et al., 2014), was used to report the certainty of identification, where level 1 is of high confidence and level 5 of low confidence. More specifically, a confidence level of 5 implies that the molecular masses of the detected feature and the potential candidate match, and a confidence level of 1 means that the spectrum of the detected feature matches that of the standard of a potential candidate. An overview of general uses was provided, where available, for features identified to at least a level 3 confidence (Haz-Map, 2021).

3. Results

3.1. Detected features, molecular weight and retention time ranges

The results, presented in Fig. 1, indicate that more positively ionisable features are present in the samples than negatively ionisable ones. The positively ionisable features are present at lower IS-eq. summed concentrations compared to the negatively ionisable ones. The differences between the positive and negative ionisation results are less pronounced for the solid phase samples than for the liquid phase ones. A higher number of positively ionisable features and a higher feature intensity is observed for the liquid phase as compared to the solid phase. However, the negatively ionisable features, the number of detected features for the negatively ionisable features is comparable for both phases.

The liquid FBW + S sample results show that the temperature and pressure conditions have a significant effect on the IS-eq. summed concentrations, but not on the detected number of features. The IS-eq. summed concentrations for the liquid phase in positive ionisation for all three test conditions significantly differ from those of the ATM_FBW + S condition. Both the HP (90 % of ATM) and the HPT_FBW + S (94 % of ATM) conditions have lower summed IS-eq. concentrations than the ATM condition, whereas the HT (109 % of ATM) condition has a higher summed IS-eq. concentration. As to the negative ionisation summed IS-eq. concentration for the liquid phase, the HPT (147 % of ATM) and the HT (118 % of ATM) conditions show a significant difference to the ATM condition, while the HP condition does not significantly differ from ATM.

The IS-eq. summed concentrations of the positive ionisation test results for the solid phase show no significant difference. A significant difference to the ATM_FBW + S sample is, however, shown by the negative ionisation results for the HPT_FBW + S (175 % of ATM) and HT_FBW + S (127 % of ATM) samples but not for HP_FBW + S.

Contrary to the liquid phase samples, the solid test samples do show a significant difference in the number of features for all three conditions in positive ionisation mode and for HT (83 % of ATM) in negative ionisation mode. The HP_FBW + S (141 % of ATM) and HT_FBW + S (66 % of ATM) samples deviate the most from the ATM_FBW + S samples in positive and negative ionisation mode, respectively.

The control samples show a different pattern from the test samples for both ionisation modes and both liquid and solid phases regarding significance and concentration changes of the HP, HT and HPT samples compared to the ATM samples. This is expected since the control samples do not include sorption and/or dissolution processes, due to the absence of shale in the FBW samples, and the absence of flowback water in the UPW + S samples. When looking at the positive ionisation results for the IS-eq. summed concentrations in the liquid phase, the FBW samples have the highest and the UPW + S samples the lowest summed IS-eq. concentrations throughout the four test conditions. One would indeed expect the lowest concentrations to occur in the UPW + S samples, since these samples contain ultrapure water and shale. The summed concentrations are, however, only slightly lower than those of the test samples. Thus suggesting that dissolution from shale to ultrapure water may have been the dominant chemical fate process in the UPW + S samples, whereas adsorption may have been dominating in the test samples.

Using negative ionisation, the test samples show the highest IS-eq. summed concentrations, followed by the FBW samples then the UPW + S samples. There are no significant differences between the FBW + S and control samples for the solid phase. The liquid FBW samples present the highest total number of detected features for the positive ionisation results. For the negative ionisation results, the total number of detected features are similar between the FBW + S and FBW samples.

In summary, the differences in IS-eq. summed concentrations of the three high pressure and temperature test samples compared to the ATM_FBW + S sample for the liquid phase, range between 90 and 109 % and 118–147 % for the positive and negative ionisation results, respectively. The differences for the solid phase test results are not significant for the positive ionisation results and range between 127 and 175 % for the negatively ionisation results. The differences in the number of features, detected in the liquid phase are not significant for neither ionisation results. These differences range between 66-141 % and 83 % for the solid phase results in positive and negative ionisation mode, respectively.

The distribution of retention times (RT) and molecular weights (MW) was assessed for the solid and liquid phase in positive (Fig. 2) and negative

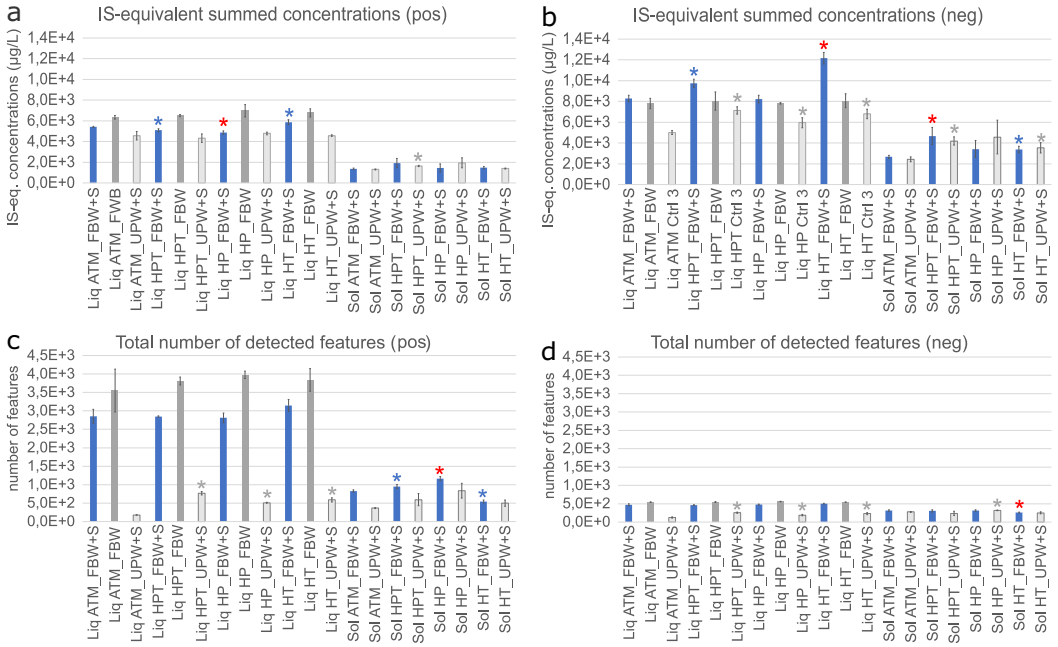

Fig. 1. Summed feature internal standard equivalent concentrations and total number of features for the positive (a, c) and negative (b, d) ionisation results in the liquid and solid phases. Concentrations are expressed as internal standard equivalent. Error bars show the standard deviations of the triplicate samples. A blue and grey asterisk represents a significant difference to the atmospheric condition for the test and control samples, respectively. A red asterisk indicates the largest significant difference to the atmospheric condition.

ionisation (Fig. A.2). For the liquid phase, both the positive and negative ionisation test results show that RT ranges for the HP and HPT conditions clearly differ from the ATM condition. The HT_FBW + S samples contain less low RT compounds than the ATM_FBW + S ones. HP and HPT conditions mainly influenced features with high retention times, and HT mainly influenced low RT features. This may indicate that HP and HPT conditions predominantly impacted sorption processes whereas HT conditions predominantly influenced degradation processes.

Regarding the RT distributions of the solid phase in positive ionisation, results show very similar ranges among the four test conditions (ATM, HP, HT and HPT), with the majority of features showing high retention times. The RT distributions of the solid phase in negative ionisation (Fig. A.2a) show very little data making it difficult to draw conclusions.

The MW distributions of the positive and negative ionisation results appear to be similar in the four conditions in the liquid phase samples. The majority of features have MWs of around 200 Da. Regarding the solid phase results for positive ionisation, the MW distributions of the four test conditions show a much higher variety than the liquid phase results. Again, the four test conditions are relatively similar, with the HP and HPT conditions differing only slightly from the ATM and HT conditions. The MW distributions of the solid phase in negative ionisation show very little data making it difficult to draw conclusions (Fig. A.2b).

In both negative and positive ionisation modes, the solid phase test conditions generally show features with higher retention times than the liquid phase test conditions. This is expected since compounds with high retention times on C18 columns are more hydrophobic and tend to have higher sorption coefficients (Krokhin et al., 2004). The positive ionisation results present similar retention times and higher molecular weights compared to the negative ionisation results. Overall, the results indicate that the compounds in the flowback water and shale are relatively small with a wide range of polarity.

3.2. Similarities and differences among the different test conditions

The principal component analysis (PCA) plots show the similarities and differences among the different test conditions for the liquid and solid phases in positive (Fig. A.3a) and negative ionisation (Fig. A.3b) modes. The dimensions 1–3 were chosen based on the scree plots (Fig. A.4a and Fig. A.4b). These three dimensions together explain 47 % and 55.4 % of the variances in positive and negative ionisation mode, respectively. Although, the solid phase results do not indicate clear differences among the different samples, the HPT_FBW + S results show slight differences with the other test conditions. For the liquid phase, differences are more pronounced. In the liquid phase the blanks, FBW and UPW + S samples cluster well together, indicating that the control samples do not show a lot of variance among the different temperature and pressure conditions. The HT_FBW + S samples in the liquid phase show the highest variance to the other test conditions. The negative ionisation results show the same trend as those of the positive ionisation results. These observations are confirmed by the hierarchical clustering results for positive and negative ionisation (Fig. A.5a and Fig. A.5b).

The volcano plots present differences between the different test conditions in positive (Fig. 3ab) and negative (Fig. A.6) ionisation. A combination of the statistical significance (y-axis) and the magnitude of change (x-axis) is plotted for each feature. The retention time is plotted as a third dimension using a color gradient from green (low) to red (high). The exact accurate mass and retention times are given for the five least intense (blue) and the five most intense (red) features.

The five least influenced features are those that remained most similar across the different conditions, and the reverse is true for the five most influenced features. The more extreme the magnitude of change (positive or negative) and the higher the significance, the larger the difference in expression for a certain feature becomes.

For the liquid phase test samples, all three conditions (HP, HT, and HPT) show similar degrees of variance to the ATM_FBW + S samples. For the solid phase, the HPT condition shows the highest variance to the ATM_FBW + S sample, which confirms the results for the solid phase shown in Fig. A.3a. Due to the relatively low number of features for the negative ionisation results, it is difficult to draw conclusions (Fig. A.6).

The ratio distributions of the IS-eq. concentrations of HP_FBW + S, HT_FBW + S and HPT_FBW + S compared to the ATM_FBW + S samples for the positively ionisable features and the negatively ionisable features are presented in Figs. 4 and A.7, respectively. The results generally show a symmetrical shape with a peak in feature percentage at a factor difference

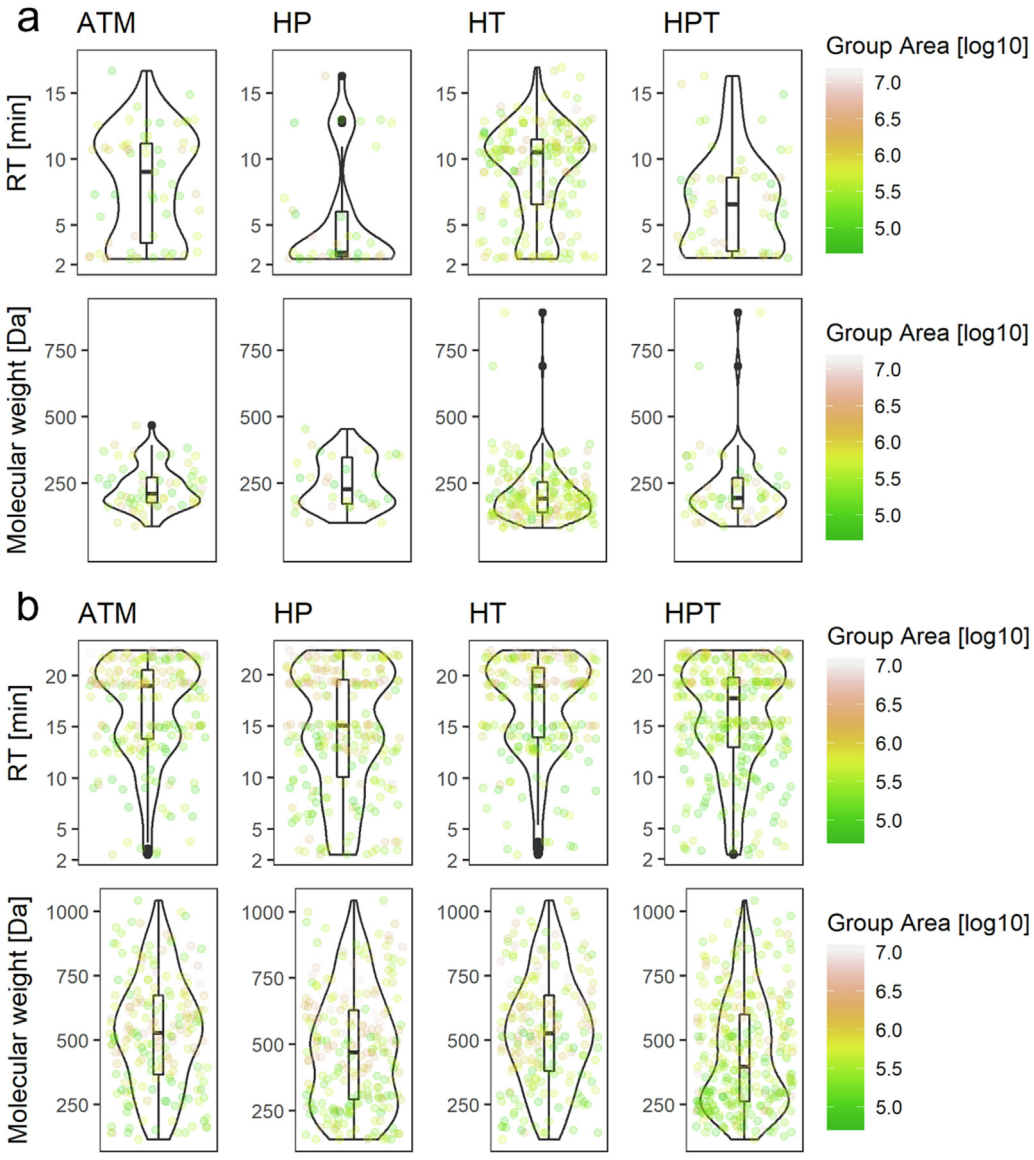

Fig. 2. Retention time and molecular weight distributions of features in positive ionisation mode for (a) the liquid phase (features with log2FC >5 between FBW + S samples and FBW samples were considered) and (b) the solid phase (features with log2FC > 5 between FBW + S samples and UPW + S samples were considered) for the four conditions.

of 1 to 5 compared to the ATM condition and a decreasing feature percentage as the factor difference increases. An exception is the solid HPT_FBW + S results for the negatively ionisable features where a more even distribution is observed (see Fig. A.7, bottom panel). This may be due to the relatively low number of features detected in this sample. The feature percentage of the positively ionisable features in the solid HP_FBW + S samples peak at a factor 2–5 (Fig. 4, top panel). Nonetheless, the results clearly show that the majority of features deviate a factor 1–5 (decrease or increase) from the ATM conditions.

3.3. Tentative identification of the five most intense features

The five features most affected by the different conditions have been tentatively identified (Tables A.2a and A.2b). Those features tentatively identified to at least a confidence level of 3 are presented in Table 2. Their uses are described here. Dibutyl phthalate is used as a plasticizer, insect repellent in textile, and as a solvent for perfumes, oils and epoxy resins (Haz-Map, 2021). It is also a geogenic compound that can be mobilised from the subsurface during hydraulic fracturing activities (Faber et al., 2017). Benzamide and Methylsuccinic acid are used in organic synthesis (Haz-Map, 2021). Glutaric acid is used in the production of polymers and for biochemical research (Haz-Map, 2021). These candidates are not specifically relevant only for hydraulic fracturing related activities. No uses were found for the other tentatively identified candidates.

3.4. Chemical fate of 1,2-benzisothiazolin-3-one under different temperature and pressure conditions

1,2-benzisothiazolin-3-one was detected in positive ionisation with a neutral molecular weight of 151 Da and a retention time of 8.81 min. The highest amount of 1,2-benzisothiazolin-3-one in the test samples was found in the liquid phase at ATM conditions (Fig. 5). The results for the three test conditions (HPT, HP and HT) are all significantly different and much lower than the ATM_FBW + S results, with the HPT (5 % of ATM) and HP (6 % of ATM) conditions deviating the most from the ATM condition.

The IS-eq. concentration of 1,2-benzisothiazolin-3-one in the solid phase is very low compared to that found in the liquid phase test results. The HP_FBW + S result is the only one significantly different from the ATM condition with an IS-eq. concentration equal to 317 % of that found

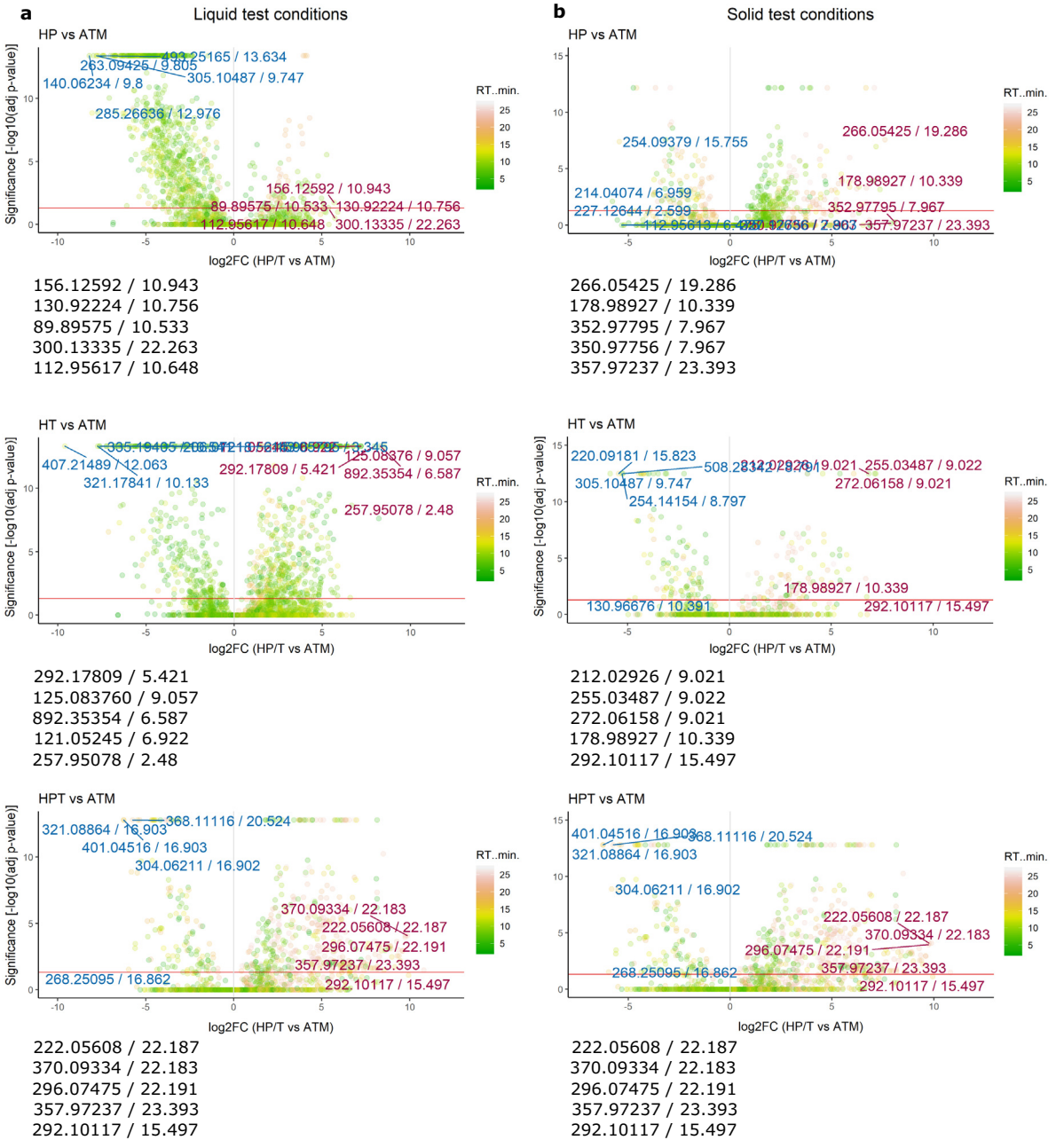

Fig. 3. Volcano plots comparing the different test conditions (HP, HT and HPT) to the atmospheric conditions for the liquid phase (a) and the solid phase (b) in positive ionisation mode. The top 5 features responsible for differences between the atmospheric and test conditions are listed at the bottom of each plot in order of importance.

in the ATM condition, indicating that dissolution occurred as a result of the high pressure conditions.

In regard to the test results, pressure had a greater impact than temperature on degradation and/or sorption processes. The results for the controls in the liquid phase did not significantly differ from the ATM control results. However, in the solid phase, all three control conditions differed significantly from the ATM control condition with the HP control sample differing the most, confirming that pressure played a major role in the chemical fate of 1,2-benzisothiazolin-3-one.

The intensity distributions of the features tentatively identified to at least a confidence level of 3 are presented in the supplementary material (Figs. A.8a-g; Table 2). In the liquid phase, HT conditions deviated the most from ATM conditions for four out of the seven tentatively identified features. One feature showed that the HP condition deviated the most and for a further two features, no significant difference was found. In the solid phase, the results of two features showed that either HT or HPT played a major role in chemical fate and the other five features showed no significant difference to the ATM condition.

3.5. Results summary

Table 3 shows a summarized overview of which test conditions deviate the most from the ATM conditions according to the different chemical properties for all retrieved features, for the spiked chemical 1,2-benzisothiazolin-3-one, and the seven tentatively identified features with a confidence level of 3. It should be noted that the tentatively identified features nr. 3 and 7 show no significant differences among the four test conditions, which is attributed to the low reproducibility of the triplicates rather than to insignificant differences from the ATM results (Fig. A.8c and Fig. A.8 g). Table 3 clearly shows that depending on what property is looked at, either temperature, pressure or the combination of both temperature and pressure play a role in chemical fate processes. These properties include

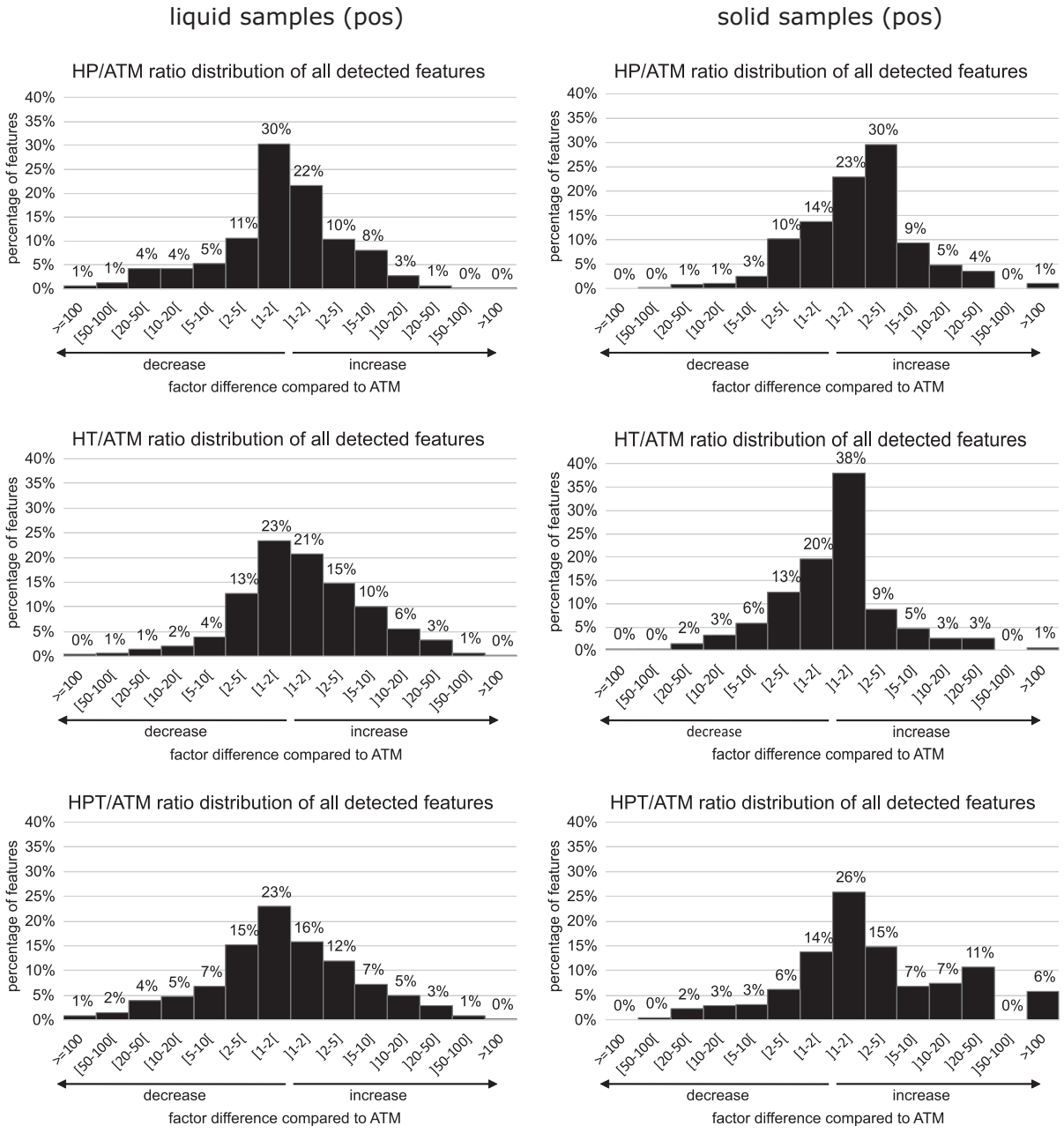

Fig. 4. Ratio distributions of the high temperature and/or pressure test samples compared to the atmospheric test samples for all the positively ionisable features detected in the liquid and solid phase samples.

Table 2
Tentative identification of the five most intense features for the different experimental conditions, with a confidence level (Schymanski et al., 2014) of at least 3.

Nr	Mode	Phase	Condition	Molecular weight (Da)	Retention time (min)	Conf. level	Molecular formula	Candidate(s)
1	pos	Liquid	HP vs ATM	278.1514	22.263	3	C16H22O4	Dibutyl phthalate
2	pos	Liquid	HT vs ATM	121.05245	6.922	3	C7H7NO	Benzamide
3	pos	Solid	HPT vs ATM; HT vs ATM	292.10117	15.497	3	C18H13FN2O	1-(4-Fluorobenzyl)-2-(2-furyl)-1H-benzimidazole 1-(2-Fluorobenzyl)-2-(2-furyl)-1H-benzimidazole
4	neg	Liquid	HT vs ATM	201.99354	2.589	3	C7H6O5S	2-Sulfobenzoic acid 4-Sulfobenzoic acid 3-Sulfobenzoic acid
5	neg	Liquid	HT vs ATM	205.97053	7.668	3	C6H6O4S2	S-(4-Hydroxyphenyl) hydrogen sulfurothioate 5-(Methylsulfonyl)-2-thiophenecarboxylic acid 5-Acetyl-2-thiophenesulfonic acid
6	neg	Liquid	HP vs ATM	132.04235	2.641	3	C5H8O4	Glutaric acid; methylsuccinic acid Methylsuccinic acid
7	neg	Solid	HT vs ATM	225.87371	3.151	3	H2O6S4	Tetrathionic acid

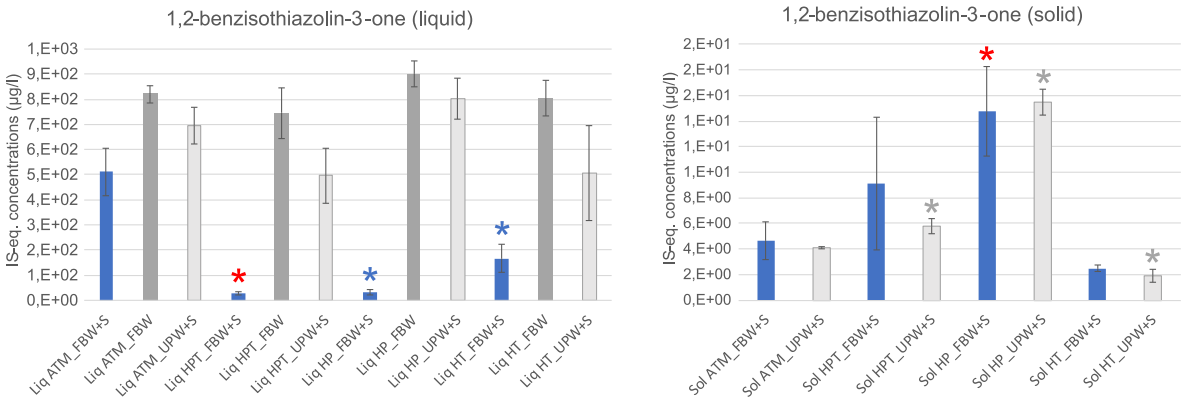

Fig. 5. Chemical fate of 1,2-benzisothiazolin-3-one under different temperature and pressure conditions in the liquid and solid phase (positive ionisation). Concentrations are expressed as internal standard equivalent. Error bars show the standard deviations of the triplicate samples. A blue and grey asterisk represents a significant difference to the atmospheric condition for the test and control samples, respectively. A red asterisk indicates the largest significant difference to the atmospheric condition for the test results.

number of chemical compounds, summed IS-eq. concentrations, molecular weight distributions, retention time distributions but also the mode in which the chemical ionises and the initial phase (solid or liquid) in which the compound is present. When looking at the total number of compounds and the summed IS-eq. concentrations, temperature and/or pressure may play a significant role in chemical fate, which leads to an increase or decrease in the number of compounds and/or their concentrations.

4. Discussion and conclusion

The results show that high temperature and/or pressure conditions impact the chemical fate of hydraulic fracturing chemicals, as can be explained by processes of transformation, sorption, degradation and/or dissolution. It is, however, not possible to clearly discern between these processes. Downhole conditions may impact possible exposure to these chemicals, and thus influence the resulting risks for humans and ecosystems (Schout et al., 2018, 2019). It is, however, also unclear to what extent temperature and/or pressure influence these processes.

The effects of pressure and/or temperature on the test samples are not comparable with those observed for the control samples. This is expected since the compounds in the FBW samples cannot undergo sorption or dissolution processes due to the absence of shale and those in the UPW + S samples do not undergo significant sorption processed due to the absence of flowback water. The conclusions based on the interpretations of the results for the compounds as a whole (Fig. 1, Fig. 2, Fig. A.2ab, Fig. 3, Fig. A.3ab and Fig. A.6) are not necessarily confirmed by the conclusions drawn from the interpretation of the results for the individual compounds (1,2-benzisothiazolin-3-one and the tentatively identified features). This may

Table 3
Test condition(s) that deviate the most from the atmospheric conditions according to the different result interpretations and the potential associated chemical fate process.

	T and P conditions significantly deviating from ATM				Potential chemical fate process
	Liquid phase		Solid phase		
	pos	neg	pos	neg	
Retention times (Fig. 2 and Fig. A.2ab)	HP; HPT	HPT; HP	ns	HP; HPT	/
Molecular weight distribution (Fig. 2 and Fig. A.2ab)	ns	ns	HPT; HT	HPT; HT	/
PCA (Fig. A.3ab)	HT	HT	HPT	ns	/
Volcano plots (Fig. 3 and Fig. A.6)	similar	nd	similar	nd	
Number of features (Fig. 1)	ns	ns	HP(141 %); HT (66 %); HPT(115 %)	HT(83 %)	/
Summed IS-eq. concentrations (Fig. 1)	HP(90 %); HT (109 %); HPT(94 %)	HT(147 %); HPT(118 %)	ns	HPT(175 %); HT (127 %)	/
1,2-benzisothiazolin-3-one (Fig. 5)	HPT(5 %); HP(6 %); HT(33 %)	/	HP (317 %)	/	Degradation (liquid) and/or sorption to shale and/or transformation (solid)
Tentatively identified feature nr. 1 (Fig. A.8a)	HP(474 %); HPT (405 %)	/	ns	/	Dissolution from shale and/or transformation (liquid)
Tentatively identified feature nr. 2 (Fig. A.8b)	HT(14,558 %); HPT (3884 %)	/	HPT(970 %); HT (622 %)	/	Transformation (liquid and solid)
Tentatively identified feature nr. 3 (Fig. A.8c)	ns	/	ns	/	nd
Tentatively identified feature nr. 4 (Fig. A.8d)	/	HT(212,728 %); HPT (40,557 %); HP(1343 %)	/	ns	Transformation (liquid) and/or dissolution
Tentatively identified feature nr. 5 (Fig. A.8e)	/	HT(60,199 %); HPT (2209 %); HP(112 %)	/	HT(5055 %); HPT(2209 %)	Transformation (liq + sol)
Tentatively identified feature nr. 6 (Fig. A.8f)	/	HT(16,780 %); HP(9854 %)	/	ns	Transformation (liquid)
Tentatively identified feature nr. 7 (Fig. A.8 g)	/	ns	/	ns	nd

ns = no significant difference among the four test conditions.
similar = the HPT, HP and HT results all deviate to the same degree from the ATM results.
nd = not determined due to inconclusive results.
/ = not relevant.

be explained by the fact that temperature and pressure have a chemical-specific effect on environmental fate processes. High pressure and/or temperature may impact chemical fate by increasing or decreasing the concentrations of compounds present in the related water and shale. Furthermore, the results show that the degree and direction of change is chemical specific, lower or equal to a factor of five compared to ATM. For a few individual compounds the degree of change can exceed this factor of five. This suggests that environmental fate models based on surface conditions may be used for an approximation of chemical fate under downhole conditions by applying an additional factor of five to account for this uncertainty, resulting in higher predicted environmental concentrations and thus more stringent standards or allowed emissions. The results thereof should, however, be interpreted by considering that this uncertainty is related to the assessment over the chemicals in general and that the results will not be representative for all compounds individually.

The available studies that investigated downhole transformation of chemicals (Kahrilas et al., 2016; Tasker et al., 2016; Xiong et al., 2018; Schenk et al., 2019; Song et al., 2022, Tables A.5 and 4) looked at chemical behaviour under downhole conditions, and generally found that temperature played a significant role whereas the effects of pressure were either negligible or not considered (Table 4). However, Song et al. (2022) found that pressure had a greater effect on methane solubility in oil-based muds than temperature did, and is the only study concluding that pressure influences downhole transformation, which is in line with the results observed in the present study. The present study found that both temperature and pressure played a role in downhole transformation of flowback related chemicals. Among the various studies used for comparison, Schenk et al. (2019) and Song et al. (2022) are the least comparable with the current study because the mediums used and research questions greatly differ from those of the current study (Tables A.5 and 4). Song et al. (2022) looked at the solubility of a gas (i.e. methane) in oil-based muds while Schenk et al. (2019) looked at the effects of high temperature on formaldehyde leaching from proppants. The current study looked at overall chemical fate in water and in shale using proxies (RT, MW, feature intensity, total number of features, IS-eq. concentrations, and similarities and differences among samples). The quality of flowback water, such as pH, salinity and dissolved organic carbon can substantially vary depending on the composition of the initially injected fracturing fluid and on the properties of the hydraulic fractured formation. These properties are important since they can influence the outcome of an experiment, and should be considered both for future studies looking to replicate the current study and for comparing results of different studies. This is also true for shale properties, such as carbon content and specific surface area.

Table A.5 shows that the mediums used and their properties vary considerably among the different studies (Kahrilas et al., 2016; Tasker et al., 2016; Xiong et al., 2018; Schenk et al., 2019; Song et al., 2022). The fluid and shale properties were not always available, and different studies reported different types of properties. The fluids used include drilling muds (Song et al., 2022). The pH strongly affects aqueous solubility of many ionisable compounds (Msaky and Calvet, 1990; Kale et al., 2020; Sirianni et al., 2021). High salinity may increase adsorption potential of certain chemicals (Diraki et al., 2022; Goh et al., 2022) and decrease solubility of organic compounds (Xie et al., 1997). The variations in medium properties among the different studies (Table A.5) can significantly impact the experimental outcomes. The different mediums used in these experiments are flowback water (current study), synthetic hydraulic fracturing fluid (Tasker et al., 2016; Xiong et al., 2018), 500 mg/L glutaraldehyde solution (Kahrilas et al., 2016), produced water (Schenk et al., 2019) and oil-based muds (Song et al., 2022). Except for the synthetic hydraulic fracturing fluid used in Tasker et al. (2016) and Xiong et al. (2018), and based on the available information, fluid properties differ greatly from each other. The specific chemical composition is only known for the fluid used in Kahrilas et al. (2016). Nonetheless due to the variety of experimental fluids used, it can be assumed that their chemical composition varies noticeably.

Table 4 clearly shows that research questions, variables and experimental properties vary among the studies used for comparison. Kahrilas et al. (2016) included the most variables in their experiment whereas Schenk et al. (2019) considered the least variables. Temperature is the only variable that was considered in all the studies. Pressure was not taken into consideration in Schenk et al. (2019). Salinity was included in Kahrilas et al. (2016) and Xiong et al. (2018). The amount of shale as a variable was included in Kahrilas et al. (2016) and Tasker et al. (2016). pH was only considered by Kahrilas et al. (2016). Higher pressures were used in the current study (450 bar) and in Song et al. (2022; 560 bar) than in the other studies (83–110 bar). These two studies were also the only ones where pressure was found to have a significant impact on the experimental outcome. High temperature conditions among the various experiments vary less than pressure (80–140 °C), with Kahrilas et al. (2016) and Song et al. (2022) using the highest temperature conditions (140 °C), followed by that of the current study (100 °C), Schenk et al. (2019; 93 °C), Tasker et al. (2016; 80 °C) and Xiong et al. (2018; 80 °C). Except for Song et al. (2022), temperature played a significant role in the experimental

Table 4
Research topics, variables and experimental properties of the current study and of the publications used for comparison purposes (Kahrilas et al., 2016; Tasker et al., 2016; Xiong et al., 2018; Schenk et al., 2019; Song et al., 2022.

Study	Research topic description	Variables considered	Variable(s) that had a significant impact	Experimental properties					
				Temperature (°C)	Pressure (bar)	pH	Salinity	Shale (amount)	Other
Current study	Effects of downhole temperature and pressure on the fate of flowback related chemicals.	Temperature and pressure	Temperature and pressure	25, 100	1, 450	–	–	500 mg (for 7,5 mL)	–
Kahrilas et al., 2016	Effects of temperature, pressure, pH and salinity on downhole transformation of glutaraldehyde.	Temperature, pressure, pH, salinity and shale amount	Temperature, pH and salinity	65, 100, 140	6.9, 110	6, 7, 8	0, 1, 2, 2.8 M [NaCl]	0, 12, 24, 36 g (for 500 mL)	–
Tasker et al., 2016	Effects of high pressure and temperature on organic compounds.	Temperature and pressure (one variable), and shale amount	Temperature and pressure (one variable)	22, 80	1, 83	–	–	0, 5, 25, 125, 250 g (for 1 L)	–
Xiong et al., 2018	Effects of temperature, pressure and salinity on polyacrilamide degradation.	Temperature, pressure and high salinity	Temperature	80	83	–	3 M [NaCl]	5 g (for 200 mL)	–
Schenk et al., 2019	Effects of high temperature on leaching of formaldehyde from proppants.	Temperature	Temperature	93	–	–	–	1 g (for 20 mL)	–
Song et al., 2022	Effects of temperature and pressure on the solubility of methane in oil-based muds.	Temperature, pressure, base oil content, and viscosity of oil-based mud	Pressure	40-140[a]	20-560[a]	–	–	70, 80, 90 % (base oil content)	20, 41, 61, 63, 64 mPa.s (oil-based mud apparent viscosity)

[a] A range is provided due to the large number of variables.

outcomes. This is probably due to the completely different matrix used in Song et al. (2022), i.e. oil-based mud, compared to the other experiments. Kahrilas et al. (2016) were the only ones to use pH as a variable in the experiments. Salinity was only used as an experimental variable in Kahrilas et al. (2016) and Xiong et al. (2018), Kahrilas et al. (2016) found that temperature, pH and salinity played a significant role in downhole transformation of glutaraldehyde, whereas Xiong et al. (2018) only found temperature to significantly impact polyacrylamide degradation. pH and salinity should be considered as experimental variables in future studies in order to elucidate the extent to which they influence downhole chemical fate.

It should also be noted that the standard deviations observed in the present study, although in general very well acceptable, show a low reproducibility of certain triplicates (see error bars in Fig. 1, Fig. 5, and Fig. A.7a-7 g). This is especially true for the solid phase samples and has an impact on the possibilities to find significant differences between conditions. This may be explained by the many steps needed for sample treatment including ASE for the solid phase samples. Another source of uncertainty lies within the setup of the experiment. In the subsurface, shale is present as a solid unit whereas in this study shale was used in powder form. This may lead to an overestimation of sorption because of the increased surface area in the powdered shale. Moreover, flowback water was used in these experiments instead of flowback fluid, so compounds present in the flowback had already been put under high pressure and temperature conditions prior to being used in this study. This may lead to an underestimation of the effects of pressure and temperature on chemical fate in regard to the results presented in this study. In addition, the evaporation of the solid phase extracts to transfer the compounds into a water matrix suitable for HRMS analysis may have caused a loss of relatively volatile compounds, which may lead to an underestimation of geogenic or sorbed chemicals in the shale. In addition, downhole conditions were simulated using temperature and pressure as variables, missing properties such as pH and salinity. This may impact the conclusions drawn in regard to the chemical processes involved to explain the differences observed between the results of the different pressure and temperature conditions.

Toxicity testing is important in evaluating the potential threat to human and environmental health (Chapman, 1995; Krewski et al., 2009; Faber et al., 2017; Diaz-Sosa et al., 2020; Faber et al., 2021; González-Vega et al., 2022; Hossini et al., 2022). However, it is difficult to determine the toxicity of a mixture based on the chemical composition due to the effects of mixture toxicity, which may result in an increase or decrease in toxicity compared to the summed toxicities of the individual compounds (Cedergreen, 2014; Altenburger et al., 2015; Kumari and Kumar, 2020; Hamid et al., 2021; Martin et al., 2021; Chatterjee and Roy, 2022). Therefore, a study focusing on the effects of high pressure and temperature on human- and eco-toxicity may be more relevant than studying the downhole effects on chemical composition. This may not be useful in advancing environmental fate models for downhole conditions but could provide important information on toxicity in relation to downhole exposure of hydraulic fracturing related chemicals. If toxicity tests show safe toxicity levels of a fracturing fluid after being subjected to downhole conditions, then chemical fate studies may not be needed. The toxicity testing would, however, need to be carried out on a hydraulic fracturing activity specific basis.

This study and other available studies clearly show that hydraulic fracturing compounds are impacted by downhole conditions. This study also found that the majority of compounds are not greatly impacted by downhole conditions (a factor 1–5 difference for the majority of chemicals). This means that standard environmental fate models, which are generally based on aboveground conditions, could be used as a first approximation of environmental fate for a majority of compounds by applying an additional factor of five to account for this uncertainty. More accurate insight into chemical fate under downhole conditions may be gained by studying a fracturing fluid of known chemical composition and include an increased number of temperature and pressure conditions as well as other variables e.g., shale concentration, salinity and pH. An array of solutions containing a different subset of compounds may be prepared to gain better insight into mixture effects of the studied compounds under different conditions. Current environmental fate models, generally relying on aboveground conditions, may then be programmed to include chemical fate prediction of compounds under different downhole conditions. However, in view of the large number of compounds involved this will be a laborious and lengthy process. A first step may be to focus on a specific region and on representative compounds and mixtures typically used for the region of interest. To do this, more transparency may be needed from the drilling companies concerning the specific composition of the hydraulic fracturing fluids used.

CRediT authorship contribution statement

Ann-Hélène Faber: Conceptualization, Methodology, Validation, Formal analysis, Resources, Writing – original draft, Writing – review & editing, Visualization. **Andrea M. Brunner:** Methodology, Validation, Formal analysis, Resources, Writing – review & editing, Visualization. **Mariska Schimmel:** Conceptualization, Methodology, Writing – review & editing. **Paul P. Schot:** Writing – review & editing, Supervision. **Pim de Voogt:** Conceptualization, Methodology, Writing – review & editing, Supervision. **Annemarie van Wezel:** Conceptualization, Methodology, Writing – review & editing, Supervision, Project administration.

Data availability

Data will be made available on request.

Declaration of competing interest

The authors declare that they have no known competing financial interests or personal relationships that could have appeared to influence the work reported in this paper.

Acknowledgements

This work is part of the research program “Shale Gas & Water” with project number 859.14.001, which is financed by the Netherlands Organization for Scientific Research (NWO) and the drinking water companies Brabant Water, Oasen, and Waterleiding Maatschappij Limburg. Further thanks to Margo van der Kooij, Nanda Huijbens-Berg, Wolter Siegers, Alex Soontjes and Claudia Kooijman for their support and assistance during analyses and data interpretation. Additional thanks to Chris Spiers, Luuk Hunfeld, Floris van Oort and Suzanne Hangx for their help with experimental design, access to the high-pressure facilities, operating of the high pressure and temperature vessel and preparation of the Teflon tubes for the experiment.

Appendix A. Supplementary data

Supplementary data to this article can be found online at https://doi.org/10.1016/j.scitotenv.2023.163888.

References

Abdi, H., Williams, L.J., 2010. Principal component analysis. Wiley. Interdiscip. Rev. Comput. Stat. 2, 433–459.

Altenburger, R., Ait-Aissa, S., Antczak, P., Backhaus, T., Barceló, D., Seiler, T.B., Brion, F., Busch, W., Chipman, K., de Alda, M.L., de Aragão Umbuzeiro, G., Escher, B.I., Falciani, F., Faust, M., Focks, A., Hilscherova, K., Hollender, J., Hollert, H., Jäger, F., Jahnke, A., Brack, W., 2015. Future water quality monitoring—adapting tools to deal with mixtures of pollutants in water resource management. Sci. Total Environ. 512, 540–551.

Amberg, S., Sachse, V., Littke, R., Back, S., 2022. Influence of Quaternary glaciations on subsurface temperatures, pore pressures, rock properties and petroleum systems in the onshore northeastern Netherlands. Neth. J. Geosci. 101, 10.

Ayers, M., 2012. ChemSpider: the free chemical database. Ref. Rev. 7, 45–46.

Beattie, J.R., Esmonde-White, F.W., 2021. Exploration of principal component analysis: deriving principal component analysis visually using spectra. Appl. Spectrosc. 75, 361–375.

Blewett, T.A., Weinrauch, A.M., Delompré, P.L., Goss, G.G., 2017. The effect of hydraulic flowback and produced water on gill morphology, oxidative stress and antioxidant response in rainbow trout (Oncorhynchus mykiss). Sci. Rep. 7, 1–11.

Blumenschein, M., Debbeler, L.J., Lages, N.C., Renner, B., Keim, D.A., El-Assady, M., 2020. v-plots: designing hybrid charts for the comparative analysis of data distributions. Comput. Graphics Forum 3, 565–577.
Bonetti, P., Leuz, C., Michelon, G., 2021. Large-sample evidence on the impact of unconventional oil and gas development on surface waters. Science 373, 896–902.
Boschee, P., 2014. Produced and flowback water recycling and reuse: economics, limitations, and technology. Oil Gas Fac. 3, 16–21.
Brantley, S.L., Vidic, R.D., Brasier, K., Yoxtheimer, D., Pollak, J., Wilderman, C., Wen, T., 2018. Engaging over data on fracking and water quality. Science 359, 395–397.
Brunner, A.M., Bertelkamp, C., Dingemans, M.M.L., Kolkman, A., Wols, B., Harmsen, D., Siegers, W., Martijn, B.J., Oorthuizen, W.A., Ter Laak, T.L., 2020. Integration of target analyses, non-target screening and effect-based monitoring to assess OMP related water quality changes in drinking water treatment. Sci. Total Environ. 705, 135779.
Butkovskyi, A., Faber, A.H., Wang, Y., Grolle, K., Hofman-Caris, R., Bruning, H., van Wezel, A.P., Rijnaarts, H.H., 2018. Removal of organic compounds from shale gas flowback water. Water Res. 138, 47–55.
Casey, C.P., Hartings, M.R., Knapp, M.A., Malloy, E.J., Knee, K.L., 2022. Characterizing the association between oil and gas development and water quality at a regional scale. Freshw. Sci. 41, 236–252.
Cedergreen, N., 2014. Quantifying synergy: a systematic review of mixture toxicity studies within environmental toxicology. PloS One 9, e96580.
Chapman, J.C., 1995. The role of ecotoxicity testing in assessing water quality. Aust. J. Ecol. 20, 20–27.
Chatterjee, M., Roy, K., 2022. Computational modeling of mixture toxicity. In Silico Methods Pred. Drug Tox. 2425, pp. 561–587.
Di Guardo, A., Gouin, T., MacLeod, M., Scheringer, M., 2018. Environmental fate and exposure models: advances and challenges in 21st century chemical risk assessment. Environ. Sci. Process. Impacts 20, 58–71.
Diaz-Sosa, V.R., Tapia-Salazar, M., Wanner, J., Cardenas-Chavez, D.L., 2020. Monitoring and ecotoxicity assessment of emerging contaminants in wastewater discharge in the City of Prague (Czech Republic). Water 12, 1079.
Diraki, A., Mackey, H.R., McKay, G., Abdala, A., 2022. Removal and recovery of dissolved oil from high-salinity wastewater using graphene–iron oxide nanocomposites. Appl. Sci. 12, 9414.
Ellafi, A., Jabbari, H., Tomomewo, O.S., Mann, M.D., Geri, M.B., Tang, C., 2020. Future of hydraulic fracturing application in terms of water management and environmental issues: a critical review. SPE Canada Unconventional Resources Conference. OnePetro.
Faber, A.H., Annevelink, M., Gilissen, H.K., Schot, P., Rijswick, M.V., Voogt, P.D., van Wezel, A.P., 2017. How to adapt chemical risk assessment for unconventional hydrocarbon extraction related to the water system. Rev. Environ. Contam. Toxicol. 246, 1–32.
Faber, A.H., Brunner, A.M., Dingemans, M.M., Baken, K.A., Kools, S.A., Schot, P.P., de Voogt, P.D., van Wezel, A.P., 2021. Comparing conventional and green fracturing fluids by chemical characterisation and effect-based screening. Sci. Total Environ. 794, 148727.
Fontenot, B.E., Hunt, L.R., Hildenbrand, Z.L., Carlton Jr., D.D., Oka, H., Walton, J.L., Osorio, A., Bjorndal, B., Hu, Q.H., Schug, K.A., 2013. An evaluation of water quality in private drinking water wells near natural gas extraction sites in the Barnett shale formation. Environ. Sci. Technol. 47, 10032–10040.
Goh, J.Y., Goh, K.S., Yip, Y.M., Ng, C.K., 2022. High salinity enhances the adsorption of 17α-ethinyl estradiol by polyethersulfone membrane: isotherm modelling and molecular simulation. Int. J. Environ. Sci. Technol. 19, 5195–5204.
González-Vega, J.G., García-Ramos, J.C., Chavez-Santoscoy, R.A., Castillo-Quiñones, J.E., Arellano-Garcia, M.E., Toledano-Magaña, Y., 2022. Lung models to evaluate silver nanoparticles' toxicity and their impact on human health. Nanomaterials 12, 2316.
Gordalla, B.C., Ewers, U., Frimmel, F.H., 2013. Hydraulic fracturing: a toxicological threat for groundwater and drinking-water? Environ. Sci. Technol. 70, 3875–3893.
Gross, S.A., Avens, H.J., Banducci, A.M., Sahmel, J., Panko, J.M., Tvermoes, B.E., 2013. Analysis of BTEX groundwater concentrations from surface spills associated with hydraulic fracturing operations. J. Air Waste Manag. Assoc. 63, 424–432.
Habauzit, D., Lemée, P., Botana, L.M., Fessard, V., 2022. Toxicity predictions for mycotoxins: a combined in silico approach on enniatin-like cluster. Expos. Health 1, 1–17.
Hajeb, P., Zhu, L., Bossi, R., Vorkamp, K., 2022. Sample preparation techniques for suspect and non-target screening of emerging contaminants. Chemosphere 287, 132306.
Hale, S.E., Arp, H.P.H., Schliebner, I., Neumann, M., 2020. Persistent, mobile and toxic (PMT) and very persistent and very mobile (vPvM) substances pose an equivalent level of concern to persistent, bioaccumulative and toxic (PBT) and very persistent and very bioaccumulative (vPvB) substances under REACH. Environ. Sci. Eur. 32, 1–15.
Hamid, N., Junaid, M., Pei, D.S., 2021. Combined toxicity of endocrine-disrupting chemicals: a review. Ecotoxicol. Environ. Saf. 215, 112136.
Haz-Map, 2021. https://hazmap.nlm.nih.gov/ website accessed April 2021.
Hernández-Pérez, L.G., Lira-Barragán, L.F., El-Halwagi, M.M., Ponce-Ortega, J.M., 2022. Optimization of water management strategies for shale gas extraction considering uncertainty in water availability and flowback water. Chem. Eng. Res. Des. 186, 300–313.
Hintze, J.L., Nelson, R.D., 1998. Violin plots: a box plot-density trace synergism. Am. Stat. 52, 181–184.
Hollander, A., Schoorl, M., van de Meent, D., 2016. SimpleBox 4.0: improving the model while keeping it simple…. Chemosphere 148, 99–107.
Hossini, H., Shafie, B., Niri, A.D., Nazari, M., Esfahlan, A.J., Ahmadpour, M., Nazmara, Z., Ahmadimanesh, M., Makhdoumi, P., Mirzaei, N., Hoseinzadeh, E., 2022. A comprehensive review on human health effects of chromium: insights on induced toxicity. Environ. Sci. Pollut. Res. 29, 70686–70705.
Hu, K., 2020. Become competent within one day in generating boxplots and violin plots for a novice without prior R experience. Met. Prot. 3, 64.
Jafarzadegan, M., Safi-Esfahani, F., Beheshti, Z., 2019. Combining hierarchical clustering approaches using the PCA method. Expert Syst. Appl. 137, 1–10.
Jin, B., Han, M., Huang, C., Arp, H.P.H., Zhang, G., 2022. Towards improved characterization of the fate and impact of hydraulic fracturing chemicals to better secure regional water quality. Environ. Sci. Proc. Impacts 24, 497–503.
Kahrilas, G.A., Blotevogel, J., Stewart, P.S., Borch, T., 2015. Biocides in hydraulic fracturing fluids: a critical review of their usage, mobility, degradation, and toxicity. Environ. Sci. Technol. 49, 16–32.
Kahrilas, G.A., Blotevogel, J., Corrin, E.R., Borch, T., 2016. Downhole transformation of the hydraulic fracturing fluid biocide glutaraldehyde: implications for flowback and produced water quality. Environ. Sci. Technol. 50, 11414–11423.
Kale, A.R., Kakade, S., Bhosale, A., 2020. A review on: solubility enhancement techniques. Curr. Pharm Res. 10, 3630–3647.
Köhn, H.F., Hubert, L.J., 2014. Hierarchical cluster analysis. Wiley StatsRef. Statistics Reference Online, pp. 1–13.
Krewski, D., Andersen, M.E., Mantus, E., Zeise, L., 2009. Toxicity testing in the 21st century: implications for human health risk assessment. Risk Anal. Int. J. 29, 474–479.
Krokhin, O.V., Craig, R., Spicer, V., Ens, W., Standing, K.G., Beavis, R.C., Wilkins, J.A., 2004. An improved model for prediction of retention times of tryptic peptides in ion pair reversed-phase HPLC: its application to protein peptide mapping by off-line HPLC-MALDI MS. Mol. Cell. Proteom. 3, 908–919.
Kumari, M., Kumar, A., 2020. Identification of component-based approach for prediction of joint chemical mixture toxicity risk assessment with respect to human health: a critical review. Food Chem. Toxicol. 143, 111458.
Laplaza, R., Das, S., Wodrich, M.D., Corminboeuf, C., 2022. Constructing and interpreting volcano plots and activity maps to navigate homogeneous catalyst landscapes. Nat. Protoc. 17, 1–20.
Li, T., Rezaeipanah, A., El Din, E.M.T., 2022. An ensemble agglomerative hierarchical clustering algorithm based on clusters clustering technique and the novel similarity measurement. J. King Saud Univ.Comp. Inform. Sci. 34, 3828–3842.
Li, X., Mu, K., Yang, S., Wei, J., Wang, C., Yan, W., Yuan, F., Wang, H., Han, D., Kang, Z., Zeng, Q., 2022. Reduction of Rhizoctonia cerealis infection on wheat through host-and spray-induced gene silencing of an orphan secreted gene. Mol. Plant-Microbe Interact. 35, 803–813.
Liteanu, E., Spiers, C.J., 2011. Fracture healing and transport properties of wellbore cement in the presence of supercritical CO2. Chem. Geol. 281, 195–210.
Mackay, D., Paterson, S., Joy, M., 1983. A quantitative water, air, sediment interaction (QWASI) fugacity model for describing the fate of chemicals in rivers. Chemosphere 12, 1193–1208.
Mansouri, K., Grulke, C.M., Judson, R.S., Williams, A.J., 2018. OPERA models for predicting physicochemical properties and environmental fate endpoints. J. Cheminform. 10, 1–19.
Mao, G., Liu, R., Zhang, N., 2022. Predicting unknown binary compounds from the view of complex network. Found. Chem. 1–8.
Martin, O., Scholze, M., Ermler, S., McPhie, J., Bopp, S.K., Kienzler, A., Parissis, N., Kortenkamp, A., 2021. Ten years of research on synergisms and antagonisms in chemical mixtures: a systematic review and quantitative reappraisal of mixture studies. Environ. Int. 146, 106206.
Masiá, A., Campo, J., Blasco, C., Picó, Y., 2014. Ultra-high performance liquid chromatography–quadrupole time-of-flight mass spectrometry to identify contaminants in water: an insight on environmental forensics. J. Chromatogr. 1345, 86–97.
MetFrag, 2020. https://msbi.ipb-halle.de/MetFrag/ website accessed May-July 2020.
Missimer, T.M., Maliva, R.G., 2020. Hydraulic fracturing in southern Florida: a critical analysis of potential environmental impacts. Nat. Resour. Res. 29, 3385–3411.
Msaky, J.J., Calvet, R., 1990. Adsorption behavior of copper and zinc in soils: influence of pH on adsorption characteristics. Soil Sci. 150, 513–522.
Osborn, S.G., Vengosh, A., Warner, N.R., Jackson, R.B., 2011. Methane contamination of drinking water accompanying gas-well drilling and hydraulic fracturing. Proc. Natl. Acad. Sci. 108, 8172–8176.
Othman, A., Aljawad, M.S., Mahmoud, M., Kamal, M.S., Patil, S., Bataweel, M., 2021. Chelating agents usage in optimization of fracturing fluid rheology prepared from seawater. Polymers 13, 2111.
Pence, H.E., Williams, A., 2010. ChemSpider: an online chemical information resource. J. Chem. Educ. 87, 1123–1124.
Preston, T.M., Chesley-Preston, T.L., 2015. Risk assessment of brine contamination to aquatic resources from energy development in glacial drift deposits: Williston Basin, USA. Sci. Total Environ. 508, 534–545.
Qu, L., Hetland, R.D., Schlichting, D., 2022. Mixing pathways in simple box models. J. Phys. Oceanogr. 52, 2761–2772.
R Core Team, 2017. A language and environment for statistical computing. R Foundation for Statistical Computing, Vienna, Austria See https://www.R-project.org.
Reemtsma, T., Berger, U., Arp, H.P.H., Gallard, H., Knepper, T.P., Neumann, M., Quintana, J.B., Voogt, P., 2016. Mind the gap: persistent and Mobile organic compounds -water contaminants that slip through. Environ. Sci. Technol. 50, 10308–10315.
Reynolds, M.A., 2020. A technical playbook for chemicals and additives used in the hydraulic fracturing of shales. Energy Fuel 34, 15106–15125.
Rodriguez, J., Heo, J., Kim, K.H., 2020. The impact of hydraulic fracturing on groundwater quality in the Permian Basin, West Texas, USA. Water 12, 796.
Ruttkies, C., Neumann, S., Posch, S., 2019. Improving MetFrag with statistical learning of fragment annotations. BMC Bioinf. 20, 1–14.
Santos, R.D.O., Gorgulho, B.M., Castro, M.A.D., Fisberg, R.M., Marchioni, D.M., Baltar, V.T., 2019. Principal component analysis and factor analysis: differences and similarities in nutritional epidemiology application. Rev. Bras. Epidemiol. 22, e190041.
Schenk, J., Carlton, D.D., Smuts, J., Cochran, J., Shear, L., Hanna, T., Durham, D., Cooper, C., Schug, K.A., 2019. Lab-simulated downhole leaching of formaldehyde from proppants by high performance liquid chromatography (HPLC), headspace gas chromatography-vacuum ultraviolet (HS-GC-VUV) spectroscopy, and headspace gas chromatography-mass spectrometry (HS-GC-MS). Environ. Sci. Process. Impacts 21, 214–223.
Schimmel, M., Liu, W., Worrell, E., 2019. Facilitating sustainable geo-resources exploitation: a review of environmental and geological risks of fluid injection into hydrocarbon reservoirs. Earth Sci. Rev. 194, 455–471.

Schout, G., Hartog, N., Hassanizadeh, S.M., Griffioen, J., 2018. Impact of an historic underground gas well blowout on the current methane chemistry in a shallow groundwater system. Proc. Natl. Acad. Sci. 115, 296–301.
Schout, G., Griffioen, J., Hassanizadeh, S.M., de Lichtbuer, G.C., Hartog, N., 2019. Occurrence and fate of methane leakage from cut and buried abandoned gas wells in the Netherlands. Sci. Total Environ. 659, 773–782.
Schymanski, E.L., Jeon, J., Gulde, R., Fenner, K., Ruff, M., Singer, H.P., Hollender, J., 2014. Identifying small molecules via high resolution mass spectrometry: communicating confidence. Environ. Sci. Technol. 48, 2097–2098.
Schymanski, E.L., Kondić, T., Neumann, S., Thiessen, P.A., Zhang, J., Bolton, E.E., 2021. Empowering large chemical knowledge bases for exposomics: PubChemLite meets MetFrag. J. Cheminfo. 13, 19.
Seth, K., Shipman, S., McCutchan, M., McConnell, D., 2013. Maximizing flowback reuse and reducing freshwater demand: case studies from the challenging Marcellus shale. SPE Eastern Regional Meeting. Soc. Petrol. Eng.
Sirianni, Q.E., Liang, X., Such, G.K., Gillies, E.R., 2021. Polyglyoxylamides with a pH-mediated solubility and depolymerization switch. Macromolecules 54, 10547–10556.
Song, X., Sukari, B.F., Wang, L., Jiang, Z., Cai, J., Xu, Y., Huang, H., 2022. Experimental investigation on the effect of methane solubility in oil-based mud under downhole conditions. Petrophysics-the SPWLA. J. Form. Eval. Reserv. Descr. 63, 218–236.
Suciu, N., Tanaka, T., Trevisan, M., Schuhmacher, M., Nadal, M., Rovira, J., Segui, X., Casal, J., Darbra, R.M., Capri, E., 2013. Environmental fate models. In: Bilitewski, B., Darbra, M.R., Barceló, D. (Eds.), Global Risk-based Management of Chemical Additives II: Risk-based Assessment And Management Strategies. 23. Springer, Berlin Heidelberg, Berlin, Heidelberg, pp. 47–71.
Sun, Y., Wang, D., Tsang, D.C., Wang, L., Ok, Y.S., Feng, Y., 2019. A critical review of risks, characteristics, and treatment strategies for potentially toxic elements in wastewater from shale gas extraction. Environ. Int. 125, 452–469.
Tasker, T.L., Piotrowski, P.K., Dorman, F.L., Burgos, W.D., 2016. Metal associations in Marcellus shale and fate of synthetic hydraulic fracturing fluids reacted at high pressure and temperature. Environ. Eng. Sci. 33, 753–765.
Thunnissen, N.W., Lautz, L.S., Van Schaik, T.W.G., Hendriks, A.J., 2020. Ecological risks of imidacloprid to aquatic species in the Netherlands: measured and estimated concentrations compared to species sensitivity distributions. Chemosphere 254, 126604.
Tisler, S., Christensen, J.H., 2022. Non-target screening for the identification of migrating compounds from reusable plastic bottles into drinking water. J. Hazard. Mater. 429, 128331.
Tong, X., Mohapatra, S., Zhang, J., Tran, N.H., You, L., He, Y., Gin, K.Y.H., 2022. Source, fate, transport and modelling of selected emerging contaminants in the aquatic environment: current status and future perspectives. Water Res. 217, 118418.
Turley, B., Caretta, M.A., 2020. Household water security: an analysis of water affect in the context of hydraulic fracturing in West Virginia,Appalachia. Water 12, 147.
Van Bergen, F., Zijp, M., Nelskamp, S., Kombrink, H., 2013. Shale gas evaluation of the Early Jurassic Posidonia Shale Formation and the Carboniferous Epen Formation in the Netherlands. In: Chatellier, J., Jarvie, D. (Eds.), Critical Assessment of Shale Resource Plays: AAPG Memoir. 103, pp. 1–24.
Vidic, R.D., Brantley, S.L., Vandenbossche, J.M., Yoxtheimer, D., Abad, J.D., 2013. Impact of shale gas development on regional water quality. Science 340, 6134.
Wang, C., Li, J., Qiu, C., Wang, L., Su, X., Huang, P., He, N., Sun, L., Bai, Y., Li, C., Wang, Y., 2023. Multimedia fates and ecological risk control strategies of phthalic acid esters in a lake recharged by reclaimed water using the QWASI fugacity model. Ecol. Model. 475, 110222.
Wang, H., Lu, L., Chen, X., Bian, Y., Ren, Z.J., 2019. Geochemical and microbial characterizations of flowback and produced water in three shale oil and gas plays in the central and western United States. Water Res. 164, 114942.
Wang, J., Hoondert, R.P., Thunnissen, N.W., van De Meent, D., Hendriks, A.J., 2020. Chemical fate of persistent organic pollutants in the arctic: evaluation of Simplebox. Sci. Total Environ. 720, 137579.
Wang, Y., Khan, S.J., Fan, L., Roddick, F., 2020. Application of a qwasi model to produce validated insights into the fate and transport of six emerging contaminants in a wastewater lagoon system. Sci. Total Environ. 721, 137676.
Westerhoff, P., Yoon, Y., Snyder, S., Wert, E., 2005. Fate of endocrine-disruptor, pharmaceutical, and personal care product chemicals during simulated drinking water treatment processes. Environ. Sci. Technol. 37, 6649–6663.
Wollin, K.M., Damm, G., Foth, H., Freyberger, A., Gebel, T., Mangerich, A., Gundert-Remy, U., Partosch, F., Röhl, C., Schupp, T., Hengstler, J.G., 2020. Critical evaluation of human health risks due to hydraulic fracturing in natural gas and petroleum production. Arch. Toxicol. 94, 967–1016.
Xie, W.H., Shiu, W.Y., Mackay, D., 1997. A review of the effect of salts on the solubility of organic compounds in seawater. Mar. Environ. Res. 44, 429–444.
Xiong, B., Miller, Z., Roman-White, S., Tasker, T., Farina, B., Piechowicz, B., Burgos, W.D., Joshi, P., Zhu, L., Gorski, C.A., Zydney, A.L., Kumar, M., 2018. Chemical degradation of polyacrylamide during hydraulic fracturing. Environ. Sci. Technol. 52, 327–336.
Yadav, S., Sarangi, G.K., Ram Mohan, M.P., 2020. Hydraulic fracturing and groundwater contamination in India: evaluating the need for precautionary action. J. Energy Nat. Resour. Law 38, 47–63.
Yazdan, M.M.S., Ahad, M.T., Jahan, I., Mazumder, M., 2020. Review on the evaluation of the impacts of wastewater disposal in hydraulic fracturing industry in the United States. Technologies 8, 67.
Zhou, S., Peng, S., Li, Z., Zhang, D., Zhu, Y., Li, X., Hong, M., Li, W., Lu, P., 2022. Risk assessment of pollutants in flowback and produced waters and sludge in impoundments. Sci. Total Environ. 811, 152250.